Propagation of Flat-top Optical Pulses in Defective Photonic Band Gap

Sarah Bolandnazar*, and Samad Roshan Entezar

Department of Physics, University of Tabriz, Tabriz, Iran

Corresponding author email: sarahbnazar@gmail.com

Received: Sept. 10, 2023, Revised: Jan. 6, 2024, Accepted: Jan. 16, 2024, Available Online: Jan. 18, 2024 DOI: 10.61186/ijop.17.1.57

ABSTRACT— In this article, we provide a theoretical investigation into the reshaping of pulses in a one-dimensional, homogeneous, isotropic, finite-size photonic crystal with two defect lavers. We use Fourier transform to find frequency and time spectra, and transfer matrix to determine transmission spectra to find the average duration and power of the output pulse. The pulses with a carrier frequency near the defect mode center and a wide frequency spectrum, undergo the most significant reshaping. Reshaping is strongest for narrow pulses with a carrier frequency at defect mode peaks. The maximum power and duration of the output pulse of a spectrally narrow pulse are all proportional to the pulse duration and exhibit extremes at the frequencies of the defect mode peaks. The power and average duration of a spectrally wide pulse's output pulse are not affected by the carrier frequency.

KEYWORDS: Reshaping, Time Envelope, Flat-Top, Fourier Transform, Photonic Crystal, Transfer Matrix, Transmission, Defect Mode, Carrier Frequency, Duration.

I.Introduction

Pulse reshaping encompasses a broad spectrum of applications, including high-speed communications and information processing [1], optical code-division multiple-access communications [2], coherent control [3], quantum control and nonlinear spectroscopy [4, 5].

Several approaches have been developed for reshaping pulses. Asghari proposes a versatile technique that employs an optical pulse reshaping method using multi-arm ultrafast optical differentiators. This method is notable for its ability to synthesize arbitrary optical pulse shapes through the coherent overlapping of successive time derivatives of an input optical pulse [6]. Radeonychev's research has shown that pulse shaping can be achieved through the modulation of resonant absorption [7]. Brixner introduces a method for shaping femtosecond pulses, employing a frequencydomain phase shaper and optimization algorithms to compensate for phase deviations and achieve specific temporal profiles [8]. A silicon-on-insulator (SOI) planar waveguide, engineered by S. Adhikary, demonstrates the capacity to effectively transform the profile of an incident super-Gaussian optical pulse into a parabolic pulse [9]. A myriad of supplementary innovative methodologies for the shaping and manipulation of optical pulses has been scrupulously documented within the scholarly literature, substantiated by references [10-12]. Furthermore, Zhao unveils a process of selfinduced transparency that remarkably reshapes ultrashort light pulses transmitted through resonant photonic crystals (PCs,) to achieve shorter durations in the output [13].

PCs play a crucial role in manipulating light waves through their periodic and dielectric nature, effectively utilizing the interfaces between different dielectric media as light scattering centers. Optical communication and optical interconnection are critical areas of interest when it comes to the applications of PCs [14, 15]. PCs are appealing for integrated optics and applications in telecommunications because they can permit the micromanipulation

of laser light in the same manner that semiconductors control electric currents [16, 17]. It is well-established that one-dimensional periodic structures can efficiently reflect waves when the wavelength, λ , satisfies the Bragg condition $\lambda=2d$, where d represents the periodicity of the structure. The range of forbidden frequencies known as the photonic band gaps (PBGs) appear in the regions where no real solutions are possible for \vec{k} , and a forbidden window for particular frequencies occurs [18, 19]. Due to their capacity to generate PBGs, PCs have attracted significant research during the past 20 years [20-22]. Usually, when a PC's translational symmetry is compromised, defect modes will be produced. The occurrence of defect modes within the PBG is a fundamental issue connected to the PBG. To accomplish this, either a defect layer can be added to the PC or a layer can be removed from structure [23-25]. Due to electromagnetic field confinement close to the defect layer, the defect mode manifests as a narrow transmission peak in the transmission spectra. Defective **PCs** have attractive properties that make them suitable for many applications, technological including development of narrowband transmission filters [26]. How the defect modes are related to the change in the thickness of the defect layer has been studied in [27]. The applications of one dimensional (1D) PCs in time delay devices [28], high-quality filters [29], and nonlinear optical diodes [30] have received a lot of attention recently. Among them, some authors have performed analytical and numerical simulations of wave packet tunneling via 1D PCs and structured media, including pulse reshaping and output pulse time delay [31-33]. Because different spectral components of the pulse behave differently, reshaping the time spectrum is typical for transmitting wave packets [34, 35]. In Ref. [36] the reshaping of ultra-short optical pulses at a wavelength of 1.53 µm using an integrated acousto-optic tunable filter is investigated. The control over the optical pulse shape is achieved by adjusting various radio-frequency electrical signals that drive the acousto-optic filter. In reference [37], the tunneling of femtosecond optical pulses through a one-dimensional photonic crystal was studied.

Roshan Entezar examines the transformation of Gaussian laser pulses in a 1D PC with two defects, focusing on the reshaping process [38]. The reshaping of the Gaussian pulse passing through the PC containing the defect layer and the frequency and duration regions where the most reshaping occurs has been investigated in the article [39]. Temporally flat-top pulses are versatile in their applications across various fields. Petrarca's work with the SPARC photoinjector illustrates their effectiveness in reducing beam emittance [40]. Additionally, Xiao's development of a fiber-loop time-lens system has been pivotal in generating ultrashort flat-top optical pulses with enhanced controllability [41]. These pulses are also integral in high-speed optical communications, as demonstrated by Palushani [42], and play a critical role in pulse amplification and free electron lasers, as explored by Lozovoy [43]. In this article, we explore the reshaping of flat-top pulses in a 1D PC with defect layers. By using the Fourier transform and transfer matrix, we can determine the transmission spectra of the PC, frequency and time spectra of the output pulse, and analyze its average duration, and power. In addition to the deliberate methods of using PCs for pulse shaping discussed in detail above, there exists an inadvertent approach as well. Often, in optical setups, a series of elements are utilized, such as various filters composed of 1D PCs. During the manufacturing process, PCs may develop imperfections. Our research demonstrates what happens to flat-top pulses when these imperfections occur.

II. GENERAL ANALYSIS

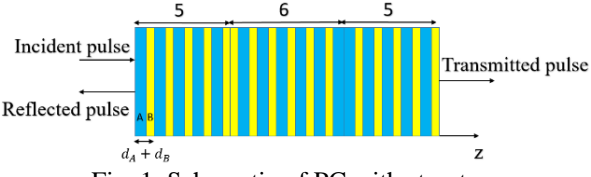


Fig. 1. Schematic of PC with structure $(AB)^5(BA)^6(AB)^5$.

We consider a one-dimensional, homogeneous, and isotropic finite-size PC with a structure

 $(AB)^5(BA)^6(AB)^5$ where A and B represent the layers with a different material and thickness Fig. 1. This structure contains two defect layers, so usually, the transmission spectra of this structure will contain two defect modes in the PBG. The flat-top pulse with the following electric field equation is projected into this crystal from the left side along the z-axis.

$$E_{i}(t) = \begin{cases} 0 & t \ge \frac{\tau_{0}}{2} \\ E_{0} & -\frac{\tau_{0}}{2} \le t \le \frac{\tau_{0}}{2} \\ 0 & t \le -\frac{\tau_{0}}{2} \end{cases} e^{-i\omega_{0}t}$$
(1)

where t, E_0 , τ_0 , ω_0 , and $E_i(t)$ are the time, electric field amplitude, duration, carrier frequency, and time envelope of the input pulse, respectively.

Using the Fourier transform, we obtain the frequency spectrum of the input pulse $E_i(\omega)$ as:

$$E_i(\omega) = \frac{1}{\sqrt{2\pi}} \int_{-\infty}^{+\infty} E_i(t) e^{i\omega t} dt.$$
 (2)

The frequency spectrum of the output pulse $(E_T(\omega))$ can be obtained as:

$$E_T(\omega) = t(\omega)E_i(\omega). \tag{3}$$

Here, $t(\omega)$ is the transmission coefficient of the structure, which can be obtained using the well-known transfer matrix method. But for the sake of brevity, we omit writing the relations related to the transfer matrix method here.

Using the Fourier transform, we obtain the time envelope of the output pulse $E_T(t)$ as follows:

$$E_T(t) = \frac{1}{\sqrt{2\pi}} \int_{-\infty}^{+\infty} E_T(\omega) e^{-i\omega t} d\omega \tag{4}$$

III.NUMERICAL RESULTS AND DISCUSSION

We assume that the considered PC consists of silicon oxide (layer A) and titanium oxide (layer B). These materials are transparent in the visible and near-infrared regimes. The refractive index of each layer is equal to $n_A = 1.45$ and $n_B = 2.47$ respectively, and the thickness of layers is equal to $d_A n_A = d_B n_B = 2.5$ µm. The first PBG and defect modes are shown in Fig. 2. As

seen in Fig. 2, the transmission spectra of this structure have two peaks.

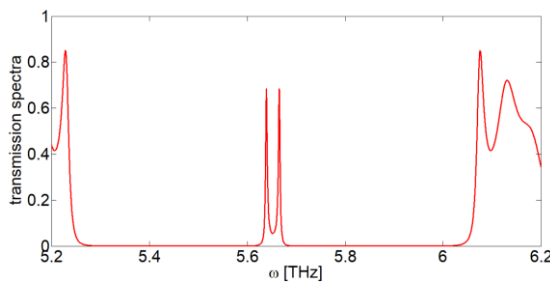


Fig. 2. PBG and defect modes.

We consider a flat-top pulse with the durations of $\tau_0 = 0.56$ ps, 5.6 ps, and the carrier frequency at the low-frequency maxima of the defect mode $\omega_l = 5.639$ THz. The normalized spectrum and the time envelope of input and output pulses are shown in Figs. 3(a) and 3(b).

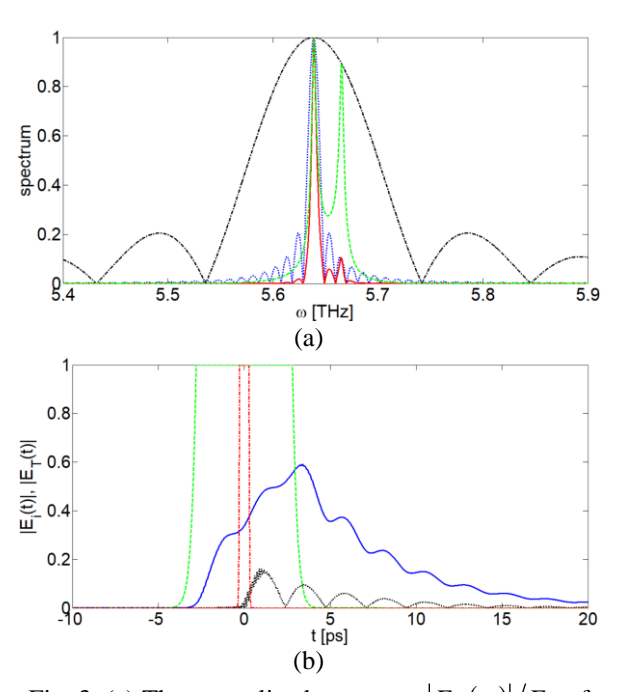


Fig. 3. (a) The normalized spectrum $|E_{in}(\omega)|/E_0$ of input pulse of duration $\tau_0=0.56$ ps (black dashdotted line) and, its normalized spectrum of output pulse $|E_{out}(\omega)|/E_0$ (green dashed line), and the normalized spectrum of input pulse of duration $\tau_0=5.6$ ps (blue dotted line), and its normalized spectrum of output pulse (red solid line) with the carrier frequency at the low-frequency maxima of the defect mode. (b) Time envelope $|E_{in}(t)|/E_0$ of the input pulse of duration $\tau_0=5.6$ ps (green dashed line) and $\tau_0=0.56$ ps (red dash-dotted line) and time envelope $|E_{out}(t)|/E_0$ of the output pulse for the duration of input pulse $\tau_0=5.6$ ps (blue solid line) and $\tau_0=0.56$ ps (black dotted line).

As seen in Fig. 3(a) and 3(b), the frequency spectrum of the flat-top pulse has a Sinc functionality. The shape of the output pulse depends on the duration of the input pulse. By reducing the duration of the input pulse, the width of the time spectrum of the input pulse becomes smaller, and as a result, its frequency width increases, which in this transmission spectrum causes the maximum time spectrum of the output pulse to decrease, and it becomes more fluctuating.

To investigate the effect of the carrier frequency on the reshaping of the output pulse, we obtain the time envelope of the output pulse as a function of the carrier frequency and time in large $\tau_0 = 5.6$ ps and small $\tau_0 = 0.56$ ps durations Fig. 4, and Fig. 5, respectively.

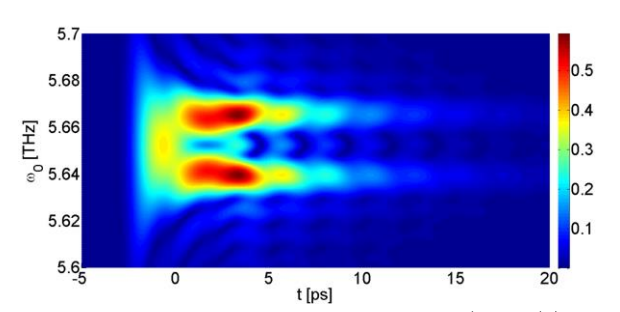


Fig. 4. Time envelope of the output pulse $|E_T(t)|/E_0$ as a function of time and carrier frequency for the duration of input pulse $\tau_0 = 5.6$ ps.

In Fig. 4, it can be seen that the maximum electric field of the output pulse is strongly dependent on the carrier frequency of the input pulse, and it has the highest value at the carrier frequency equal to the low $\omega_l = 5.639$ THz and high $\omega_h = 5.665$ THz frequency maxima of the defect mode, and it drops sharply in the other frequency areas.

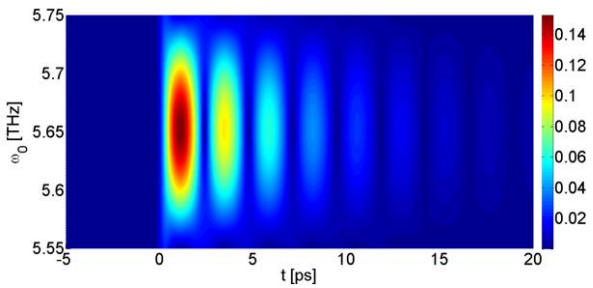


Fig. 5. Time envelope of the output pulse $|E_{out}(t)|/E_0$ as a function of the time and carrier frequency for the duration of input pulse $\tau_0 = 0.56$ ps.

In Fig. 5, it can be seen that the maximum electric field is at the carrier frequency equal to the central frequency of the defect mode $\omega_c = 5.652$ THz. It decreases slowly in other frequency regions, and its shape is approximately in fluctuating form.

To evaluate the power P_{out} and average duration of output pulse τ_{out}^{av} , we define Eq. (5), and Eq. (6).

$$P_{out} = \frac{\int |E_T(t)|^2 dt}{\int |E_i(t)|^2 dt} P_{in}$$
 (5)

where P_{in} is the power of the input pulse.

$$\tau_{out}^{av} = \frac{\int_{-\infty}^{+\infty} |E_T(t)t| dt}{\int_{-\infty}^{+\infty} |E_T(t)| dt}$$
 (6)

The average duration and power of the output pulse for two different durations are shown in Figs. 6, and 7, respectively.

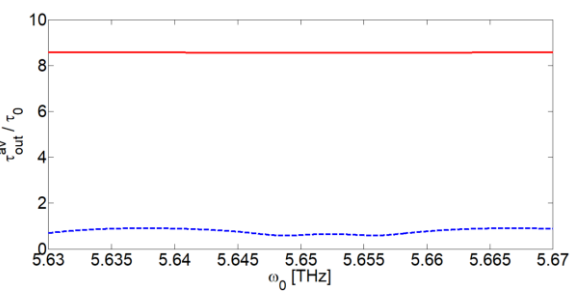


Fig. 6. Average duration of the output pulse as a function of a carrier frequency for the duration of input pulse $\tau_0 = 0.56$ ps (red solid line) and $\tau_0 = 5.6$ ps (blue dashed line).

According to Fig. 6, if the input pulse is wide in terms of time spectrum, the output pulse will be narrower, and if it is narrow, the output pulse will be wider.

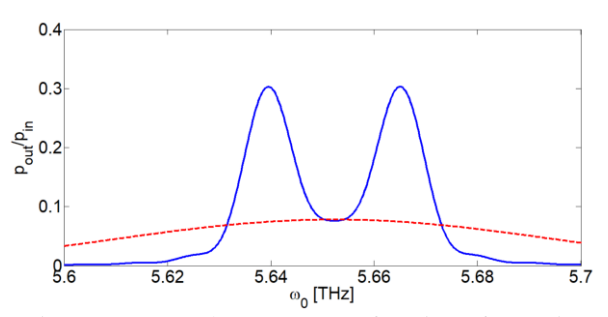


Fig. 7. Output pulse power as a function of a carrier frequency for the duration of input pulse $\tau_0 = 0.56$ ps (red dashed line) and $\tau_0 = 5.6$ ps (blue solid line).

According to Fig. 7, the power of the output pulse for the duration of the input pulse $\tau_0 = 5.6$ ps depends on the carrier frequency. It reaches its maximum value at the carrier frequency equal to ω_l and ω_h , but for duration $\tau_0 = 0.56$ ps it is relatively constant in the entire frequency range.

To investigate the effect of the pulse duration on the reshaping of the output pulse, we obtain the time envelope of the output pulse as a function of the pulse duration and time for carrier frequencies at the center and at the low-frequency maxima of the defect mode Fig. 8, and Fig. 9, respectively.

According to Fig. 8, the maximum electric field of the output pulse is in the region where the duration of the input pulse is less than 2ps, and its shape fluctuates in this area, for wider pulses, the output pulse profile is wide, and has a weak oscillation sequence.

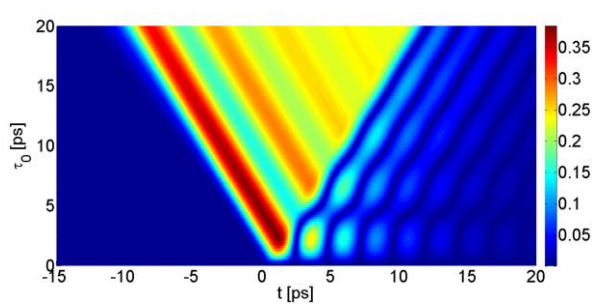


Fig. 8 Time envelope of the output pulse $\left|E_{\scriptscriptstyle out}\left(t\right)\right|/E_{\scriptscriptstyle 0}$ as a function of the input pulse duration τ_0 for carrier frequency ω_c . The color depicts the value of $\left|E_{\scriptscriptstyle out}\left(t\right)\right|/E_{\scriptscriptstyle 0}$.

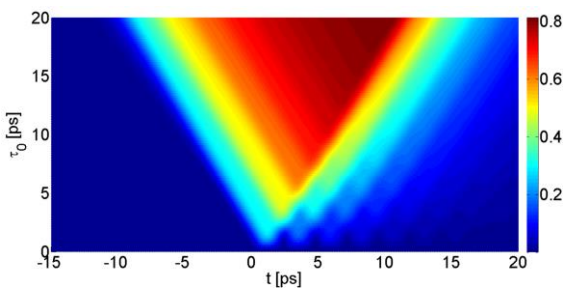


Fig. 9. Time envelope of the output pulse $|E_{\scriptscriptstyle out}(t)|/E_{\scriptscriptstyle 0}$ as a function of the input pulse duration τ_0 for carrier frequency ω_l . The color depicts the value of $|E_{\scriptscriptstyle out}(t)|/E_0$.

According to Fig. 9, for durations less than 2ps, the intensity of the electric field of the output

pulse is low, and its shape is almost fluctuating. With the increase in the duration of the input pulse, the intensity of the output pulse increases and its shape is almost like a flat-top pulse.

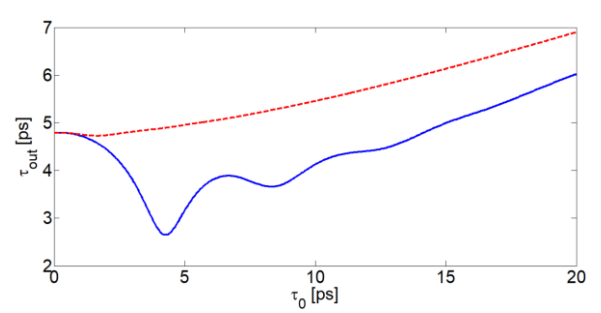


Fig. 10. Duration of output pulse as a function of the input pulse duration τ_0 for carrier frequency ω_c (blue solid line) and ω_l (red dashed line).

To check the characteristics of the output pulse, we obtain the duration and power of the output pulse as a function of the input pulse duration for carrier frequencies at the center and the low-frequency maxima of the defect mode Fig. 10, and Fig. 11.

In Fig. 10, it is clear that for the carrier frequency equal to (ω_l) , as the input pulse width increases, the output pulse width also increases. For the carrier frequency equal to (ω_c) , the output pulse width decreases until the duration of approximately 4ps and then increases.

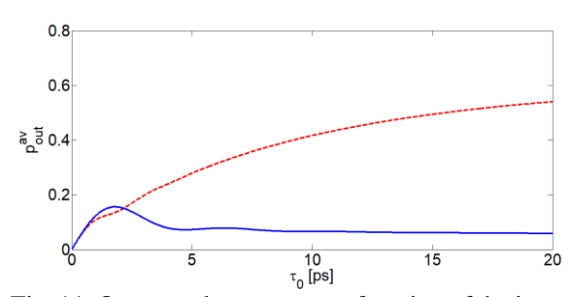


Fig. 11. Output pulse power as a function of the input pulse duration τ_0 for carrier frequency ω_c (blue solid line) and ω_l (red dashed line).

It can be seen in Fig. 11 that the power of the output pulse with the carrier frequency equal to ω_c increases with the increase in the duration of the input pulse up to approximately 2ps and then decreases. For a pulse with a carrier frequency equal to ω_l , its output power increases with increasing pulse duration.

IV. CONCLUSION

In this article, the reshaping of the flat-top pulse passing through a homogeneous and isotropic 1D PC containing two defect layers is investigated, and the effect of the carrier frequency and the duration of the input pulse on the power, and duration of the output pulse is investigated. According to the findings of this article, for a pulse with a wide frequency spectrum, the most reshaping is related to the carrier frequency near the center of the defect mode. Also, in such a case, the power, and duration of the output pulse have very little dependence on the carrier frequency of the input pulse. But for a pulse with a narrow frequency spectrum, the most reshaping is focused on the frequency areas where the carrier frequency of the input pulse is equal to the low and high-frequency maxima of the defect mode, and in such a case the power, and duration of the output pulse are strongly dependent on the carrier frequency of the input pulse.

Future research could focus on examining this phenomenon under conditions of high applied intensities, where the layers demonstrate nonlinear behavior and may potentially possess magnetic properties. This will enable an indepth exploration of the process in scenarios featuring magnetic properties.

Reshaping flat-top pulses transmitted through photonic crystals holds promising applications in advancing optical communication systems and enabling efficient manipulation of signal characteristics for enhanced information processing in diverse technological domains.

REFERENCES

- [1] A.M. Weiner and A.M. Kanan, "Femtosecond pulse shaping for synthesis, processing, and time-to-space conversion of ultrafast optical waveforms," IEEE J. Select. Topics Quantum Electron., Vol. 4, pp. 317-331, 1998.
- [2] A.M. Weiner, "Fourier information optics for the ultrafast time domain," Appl. Opt., Vol. 47, pp. A88-A96, 2008.
- [3] D. Goswami, "Optical pulse shaping approaches to coherent control," Phys. Reports, Vol. 374, pp. 385-481, 2003.

- [4] P. Nuernberger, G. Vogt, T. Brixner, and G. Gerber, "Femtosecond quantum control of molecular dynamics in the condensed phase," Phys. Chem. Chem. Phys., Vol. 9, pp. 2470-2497, 2007.
- [5] Y. Silberberg, "Quantum Coherent Control for Nonlinear Spectroscopy and Microscopy," Ann. Rev. Phys. Chemi., Vol. 60, pp. 277-292, 2009.
- [6] H.M. Asghari and J. Azana, "Proposal and analysis of a reconfigurable pulse shaping technique based on multi-arm optical differentiators," Opt. Commun., Vol. 281, pp. 4581-4588, 2008.
- [7] Y.V. Radeonychev, V.A. Polovinkin, and O.Kocharovskaya, "Pulse Shaping via Modulation of Resonant Absorption," Laser Phys., Vol. 19, pp. 769-775, 2009.
- [8] T. Brixner, A. Oehrlein, M. Strehle, and G. Gerber, "Feedback-controlled femtosecond pulse shaping," Appl. Phys., Vol. 70, pp. 119-124, 2000.
- [9] S. Adhikary and M. Basu, "Nonlinear pulse reshaping in a typically designed silicon-on-insulator waveguide and its application to generate a high repetition rate pulse train," J. Opt., Vol. 23, pp. 125506(1-12), 2021.
- [10] D.E. Leaird and A.M. Weiner, "Femtosecond direct space-to-time pulse shaping," IEEE J. Quantum Electron., Vol. 37, pp. 494-504, 2001.
- [11] D. E. Leaird, and A.M. Weiner, "Femtosecond direct space-to-time pulse shaping in an integrated-optic configuration," Opt. Lett., Vol. 29, pp. 1551-1553, 2004.
- [12] A. Vega, D.E. Leaird, and A.M. Weiner, "High-speed direct space-to-time pulse shaping with 1 ns reconfiguration," Opt. Lett., Vol. 35, pp. 1554-1556, 2010.
- [13] J. Zhao, J. Li, H. Shao, J. Wu, and J. Zhou, "Reshaping ultrashort light pulses in resonant photonic crystals," J. Opt. Soc. Am. B., Vol. 23, pp. 1981-1987, 2006.
- [14] J. Lumeau, L.B. Glebov, and V. Smirnov, "Tunable narrowband filter based on a combination of Fabry-Perot etalon and volume Bragg grating," Opt. Lett., Vol. 31, pp. 2417-2419, 2006.
- [15] S.W. Shao, X.S. Chen, W. Lu, M. Li, and H.Q. Wang, "Fractal independently tunable

- multichannel filters," Appl. Phys. Lett., Vol. 90, pp. 211113(1-3), 2007.
- [16] S. John, O. Toader, and K. Busch, *Photonic Band Gap Materials: Semiconductors of Light, Encyclopedia of Physical Science and Technology*, edited by Robert A. Meyers Academic Press, San Diego, Vol. 12, p. 133, 2002.
- [17] E. Yablonovitch, "Photonic crystals: semiconductors of light," Sci. Am. Mag., Vol. 285, pp. 46-51, 54-55, 2001.
- [18] J.D. Joannopoulos, *Photonic crystals: Molding the flow of light*, Princeton University Press, 2008.
- [19] E. Yablonovitch. "Photonic band-gap structures," J. Opt. Soc. Am. B, Vol. 10, pp. 283-295, 1993.
- [20] J.D. Joannapoulos, S.G. Johnson, J.N. Winn, and R.D. Meude, *Photonic crystals: modeling the flow of light*, Princeton University Press, USA, 2011.
- [21] I.L. Lyubchanskii, N.N. Dadoenkova, M.I. Lyubchanskii, E.A. Shapovalov, and Th. Rasing, "Magnetic photonic crystals," J Phys. D: Appl. Phys., Vol. 36, pp. R277–R287, 2003.
- [22] K. Inoue and K. Ohtaka, *Photonic Crystals: Physics, Fabrication and Applications*, Springer Science & Business Media, Vol. 94, 2004.
- [23] C.-J. Wu and Z.H. Wang, "Properties of defect modes in one-dimensional photonic crystals," Prog. Electromag. Research, Vol. 103, pp. 169-164, 2010.
- [24] S.K. Srivastava, M. Upadhyay, S.K. Awasthi, S.P. Ojha, "Tunable Reflection Bands and Defect Modes in One-Dimensional Tilted Photonic Crystal Structure," Opt. Photon. J., Vol. 2, pp. 230-236, 2012.
- [25] H.Y. Liu, S. Liang, Q.-F. Dai, L.-J. Wu, S. Lan, A.V. Gopal, V.A. Trofimov, T. M. Lysak, "Transmission of terahertz wave through one-dimensional photonic crystals containing single and multiple metallic defects," J. Appl. Phys., Vol. 110, pp. 073101, 2011.
- [26] E. Yablonovitch, T.J. Gmitter, R.D. Meade, A.M. Rappe, K.D. Brommer, and J.D. Joannopoulos, "Donor and acceptor modes in photonic band structure," Phys. Rev. Lett., Vol. 67, pp. 3380–3383, 1991.

- [27] T.-C. King and C.-J. Wu, "Properties of defect modes in one-dimensional symmetric defective photonic crystals," Physica E, Vol. 69, pp. 39-46, 2015.
- [28] A.M. Steinberg and R.Y. Chiao, "Subfemtosecond determination of transmission delay times for a dielectric mirror (photonic band gap) as a function of the angle of incidence," Phys. Rev. A, Vol. 51, pp. 3525-3528, 1995.
- [29] T. Hattori, N.T. Surumachi, and H. Nakatsuka, "Analysis of optical nonlinearity by defect states in one-dimensional photonic crystals," J. Opt. Soc. Am. B., Vol. 14, pp. 348–355, 1997.
- [30] M.D. Tocci, M.J. Bloemer, M. Scalora, J.P. Dowling, and C.M. Bowden, "Thin-film nonlinear optical diode," Appl. Phys. Lett., Vol. 66, pp. 2324–2326, 1995.
- [31] H. Winful, "Tunneling time, the Hartman effect, and superluminality: a proposed resolution of an old paradox," Phys. Rep., Vol. 436, pp. 1–69, 2006.
- [32] S. Doiron, A. Haché, and H.G. Winful, "Direct space-time observation of pulse tunneling in an electromagnetic band gap," Phys. Rev. A., Vol. 76, pp. 023823(1-6), 2007.
- [33] P. Pereyra and H.P. Simanjuntak, "Time evolution of electromagnetic wave packets through superlattices: evidence for superluminal velocities," Phys. Rev. E., Vol. 75, pp. 056604(1-7), 2007.
- [34] Yu. F. Nasedkina and D. I. Sementsov, "Gaussian pulse transformation upon reflection from a resonant medium," Opt. Spectrosc., Vol. 104, pp. 591–596, 2008.
- [35] I.O. Zolotovski i, R.N. Minvaliev, and D.I. Sementsov, "Parametric interaction and compression of optical pulses in field of high-power pump wave," Opt. Spectrosc., Vol. 109, pp. 584–589, 2010.
- [36] M.E. Fermann, V. da Silva, D.A. Smith, Y. Silberberg, and A.M. Weinee, "Shaping of ultrashort optical pulses by using an integrated acousto-optic tunable filter," Opt. Lett., Vol. 18, pp. 1505–1507, 1993.
- [37] Ch. Spielmann, R. Szipöcs, A. Stingl, and F. Krausz, "Tunneling of optical pulses through photonic band gaps," Phys. Rev. Lett., Vol. 73, pp. 2308–2311, 1994.

- [38] S. Roshan Entezar, "Reshaping of Gaussian light pulses via defective nonlinear one-dimensional photonic crystals," Opt. Laser Technol., Vol. 164, pp. 109508(1-5), 2023.
- [39] YU.S. Dadoenkova, N.N.D Dadoenkova, I.L. Lyubchanskii, and D.I. Sementsov, "Reshaping of Gaussian light pulses transmitted through one-dimensional photonic crystals with two defect layers," Appl. Opt., Vol. 55, pp. 3764-3770, 2016.
- [40] M. Petrarca, P. Musumeci, M.C. Mattioli, C. Vicario, G. Gatti, A. Ghigo, S. Cialdi, and I. Boscolo, "Production of temporally flat-top UV laser pulses for SPARC photo-injector," International Conference on Charged and Neutral Particles Channeling Phenomena, Vol. 6634, 2006.
- [41] H. Xiao, C. Huang, J. Xu, and Y. Tang, "Generating ultrashort flat-top optical pulses with a fiber-loop time-lense system," Int. J. Light Electron Opt. (Optik), Vol. 185, pp. 287-293, 2019.
- [42] E. Palushani, L.K. Oxenlowe, M. Galili, H.C. H. Mulvad, A.T. Clausen, and P. Jeppesen, "Flat-top pulse Generation by the Optical Fourier Transform Technique for Ultrahigh Speed Signal Processing,' IEEE J. Quantum Electron., Vol. 45, pp. 1317-1324, 2009.
- [43] V. Lozovoy, G. Rasskazov, A. Ryabtsev, and M. Dantus, "Phase-only synthesis of ultrafast stretched square pulses," Opt. Express, Vol. 23, pp. 27105-27112, 2015.



Sarah Bolandnazar was born in Tabriz, Iran, in 1997. She received her BSc degree in physics and MSc degree in laser physics from University of Tabriz, Tabriz, Iran, in 2020 and 2023, respectively.

Her current research activities are in the fields of quantum optics in photonic crystals, the linear and nonlinear optics in photonic crystals.



Samad Roshan Entezar was born in Tabriz, Iran, in 1969. He received his MSc degree in physics (atomic and molecular) and PhD degree in laser physics from University of Tabriz, Tabriz, Iran, in 2001 and 2006, respectively. In 2007, he joined the Physics Department of University of Tabriz as an assistant professor of Physics. His current research activities are in the fields of quantum optics in photonic crystals, the linear and nonlinear optics in photonic crystals and metamaterial. Dr. Roshan Entezar has authored and co-authored more than 82 scientific papers in peer-reviewed international journals.